Optical vortices with large orbital momentum: generation and interference

Anatoliy A. Savchenkov[1], Andrey B. Matsko[1], Ivan Grudinin[1], Ekaterina A. Savchenkova[2], Dmitry Strekalov[1], and Lute Maleki[1]

[1] *Jet Propulsion Laboratory, California Institute of Technology, MS 298-100, 4800 Oak Grove Drive, Pasadena, CA 91109-8099*

[2] *Moscow Lomonosov State University, Department of Physics, Vorob'evy Gory, Moscow, 119992, Russia*

Andrey.Matsko@jpl.nasa.gov

Abstract: We demonstrate a method for generation of beams of light with large angular momenta. The method utilizes whispering gallery mode resonators that transform a plane electromagnetic wave into high order Bessel beams. Interference pattern among the beams as well as shadow pictures induced by the beams are observed and studied.

OCIS codes: (230.5750) Resonators, (260.1960) Diffraction theory, (140.3300) Laser beam shaping

References and links

1. L. Allen, M. J. Padgett, and M. Babiker, "The orbital angular momentum of light", Progress in Optics **39**, 291-372 (1999).
2. L. Allen, "Introduction to the atoms and angular momentum of light special issue," J. Opt. B **4**, S1-S6 (2002).
3. E. Santamato, "Photon orbital angular momentum: problems and perspectives," Progress in Physics **52**, 1141-1153 (2004).
4. D. McGloin and K. Dholakia, "Bessel beams: diffraction in a new light," Contemp. Phys. **46**, 15-28 (2005).
5. J. Courtial, K. Dholakia, L. Allen, and M. J. Padgett, "Gaussian beams with very high orbital angular momentum," Opt. Commun. **144**, 210-213 (1997).
6. J. E. Curtis, B. A. Koss, and D. G. Grier, "Dynamic holographic optical tweezers," Opt. Commun. **207**, 169-175 (2002).
7. S. Sundbeck, I. Gruzberg, and D. G. Grier, "Structure and scaling of helical modes of light," Opt. Lett. **30**, 477-479 (2005).
8. A. B. Matsko, A. A. Savchenkov, D. Strekalov, and L. Maleki, "Whispering gallery resonators for studying orbital angular momentum of a photon," Phys. Rev. Lett. **95**, 143904 (2005).
9. E. J. Galvez, P. R. Crawford, H. I. Sztul, M. J. Pysher, P. J. Haglin, and R. E. Williams, "Geometric phase associated with mode transformations of optical beams bearing orbital angular momentum," Phys. Rev. Lett. **90**, 203901 (2003).
10. F. Gori, G. Guattari, and C. Padovani, "Bessel-Gauss beams," Opt. Commun. **64**, 491-495 (1987).
11. L. Landau and E. Lifshitz, *Classical Theory of Fields* (Reed International Educational and Professional Publishing, Oxford, 1980).

1. Introduction

Optical vortices or light beams with nonzero angular momenta are interesting not only because of their underlying physics, but also because of their potential applications. Generation of such vortices and the study of their properties has recently attracted considerable attention. The beams have been realized with both passive and active schemes (see [1, 2, 3, 4] for review). Nonetheless, generation of beams with orbital angular momentum exceeding $10^4\hbar$ per photon,

#67784 - $15.00 USD Received 6 February 2006; revised 28 March 2006; accepted 29 March 2006

though in principle possible, [5], is not easily achievable experimentally. To our knowledge, the highest orbital angular momenta of photons observed thus far are approximately $25\,\hbar$ [5] and $30\hbar$ [6]. Beams with angular momenta up to $300\,\hbar$ were recently demonstrated [7]. In this paper we discuss another method for the generation of photons with large orbital momentum.

We report on a proof of principle experiment validating the application of a low contrast whispering gallery mode (WGM) resonator that supports modes with high angular momenta for the generation of high-order Bessel beams [8]. By "low contrast" we mean a new design whereby the resonator is a part of the waveguide, but has a slightly different radius than the waveguide. The resonator can be made by cutting and polishing a bump or dip pattern on the waveguide surface. Such a resonator has an important distinction from the ordinary WGM resonators since its modes decay primarily into Bessel modes of the waveguide, and not to the outside environment. By changing the resonator shape and the radius of the waveguide it is possible to change the resonator loading and to allow light propagation from the resonator to the waveguide.

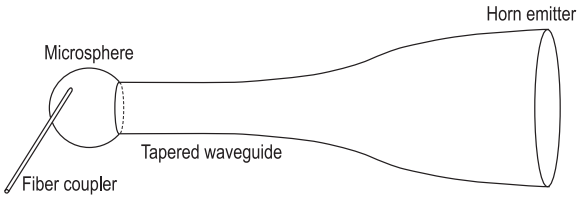

Fig. 1. Scheme of the experiment.

The feasibility of the applications of the optical waves possessing angular momenta directly depends on their propagation distance in the free space. A high order running Bessel wave that penetrates into a cylindrical waveguide from the resonator through evanescent field coupling cannot leave the waveguide. It runs until the end of the waveguide and reflects, because of the total internal reflection. It is possible to manipulate the wave inside the waveguide. However, the complete confinement of the waves in the waveguide reduces the spectrum of their applications. We used a tapered waveguide to release the Bessel beam into free space.

We have been able to generate Bessel beams with orders exceeding a thousand, and have studied interference of multiple beams with different angular momenta as well as pictures of shadow of an object placed in front of them. The shadow has properties that arise from the far field interference of the beams of different orders at different points at the exit of the waveguide. This interference experiment allowed us to estimate the propagation distance of the optical vortices. The distance drastically decreases with an increase of the value of the angular momentum. We explain the results theoretically and discuss the possibility of increasing the propagation distance. The experiments with shadows have shown that a shadow of a straight rod illuminated with a Bessel beam is not a straight line. This result is explained theoretically in the frame of geometrical, not wave, optics.

2. Experiment

We fabricated several low contrast fused silica WGM resonators being integral parts of tapered waveguides (Fig. 1). In one experiment, a segment of a fused silica multimode fiber rod is cleaved and the cleavage plane is polished. The diameter of the fiber is 1 mm. The other end of the rod is stretched into a conical shape in a hydrogen burner. This end is fused to form a WGM resonator having about 300 μm in diameter as an integral part of a cone. This cone starts at the WGM at diameter of about 250-280 μm and expands to 1 mm in diameter over 1 cm distance

#67784 - $15.00 USD Received 6 February 2006; revised 28 March 2006; accepted 29 March 2006

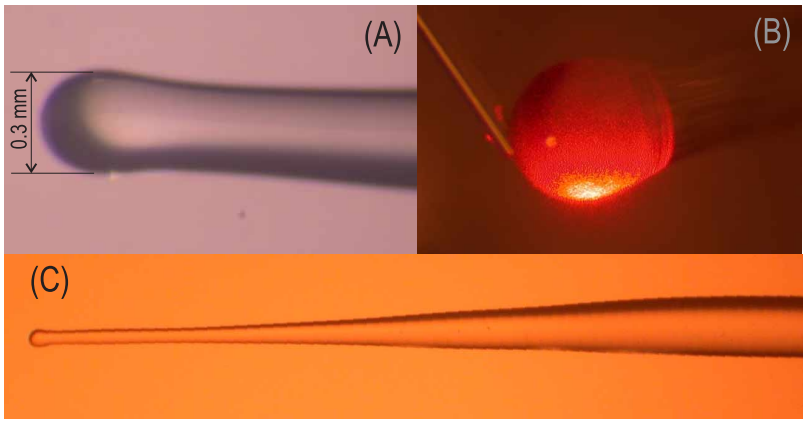

Fig. 2. A low contrast whispering gallery mode resonator for a Bessel beam generation. The resonator is created by the local increase of the waveguide radius. A tapered waveguide is used to generate a Bessel beam in the free space. Increasing the waveguide radius changes the wave vector of the light, guaranteeing escape of the light from the waveguide into free space. (A) A low contrast fused silica WGM resonator attached to the tapered waveguide. (B) Coupling light into the WGMs of the resonator using cleaved fiber. (C) Tapered fiber used to release generated Bessel beam into free space.

(Fig. 2). Another resonator we built has a 500 μm diameter, and the taper diameter changes from 450 μm to 3 mm over a 3 cm distance.

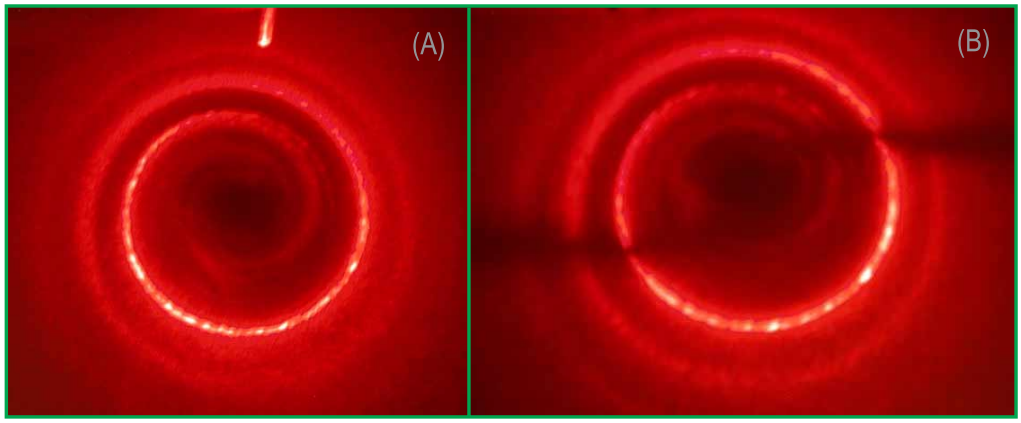

Fig. 3. (A) Far field interference pattern of multiple copropagating Bessel beams. (B) Far field shadow of a 250 μm-thick needle placed to the beam emerging the fiber taper.

The resonators were optically pumped with 650 nm light using an angle polished fiber coupler. We excited a family of WGMs that interacted with the modes of the tapered fiber. The fiber coupler is shown in (Fig. 2(B)). It is easy to see the glow on the resonator surface resulting from the scattering of the light in the WGMs, which abruptly disappears in the vicinity of the coupling point between the resonator and the tapered fiber. This glow shows the geometrical localization of light in the resonator.

#67784 - $15.00 USD Received 6 February 2006; revised 28 March 2006; accepted 29 March 2006

As the WGMs of the resonator decay into the fiber, light propagates and exits the fiber into the free space as truncated Bessel beams. Because the ratio of the taper entrance over the exit diameters was small ($r_{exit}/r_{entrance} = 6$ or less) and the mode order was high ($> 10^3$), the propagation distance of Bessel beams in free space did not exceed ten millimeters. The beams spread out creating peculiar interference shapes in the far field region (Fig. 3(A)). This observation has a certain similarity with the interference pattern of zero and first order Laguerre-Gauss beams presented in [9]. In what follows it is shown that in our case the interference occurs between multiple high-order truncated Bessel beams.

Aside from the interference we have observed peculiar shapes of the shadow of a straight, thin, opaque object parallel to the waveguide surface that crosses the symmetry axis of the beam possessing large angular momentum (Fig. 3(B)) (also see Fig. 9 for more details of the experiment). To generate the shadow we used a 250 μm needle as the object. The shadow is orthogonal to the object in the center of the interference pattern, and is parallel, but displaced, far from the center. The shape of the shadow depends on the distance of the object from the surface of the taper. The closer the wire is, the longer is the region of the orthogonal shadow. We have repeated the same experiment using 532 nm laser and a 25 μm thick piece of a tungsten wire, and obtained similar result. The dynamics of the behavior of the shadow with the distance change is demonstrated in Fig. 4. In what follows we explain the result of the experiment

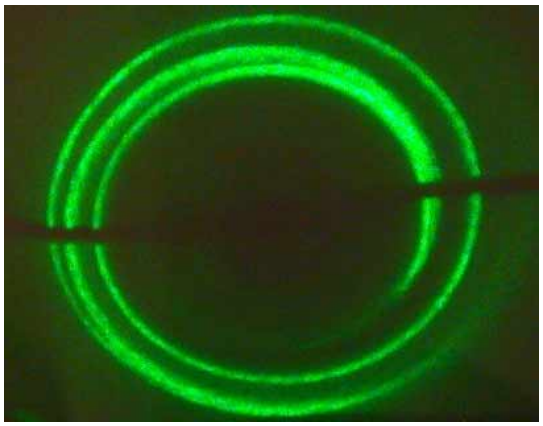

Fig. 4. (0.7 Mb) Movie. A shadow of a straight wire illuminated with the light possessing large angular momentum. The distance between the wire and the waveguide surface changes from 12.5 mm to zero. Two mixed interference patterns come from two polarizations of the light.

theoretically.

3. Theory

3.1. Interference

The interference pattern (Fig. 3) could be explained if we consider the interference of multiple radially truncated high order Bessel waves with nearly the same diameter but different angular momenta. Light from an angle polished fiber coupler (Fig. 2(B)) excites many modes of the resonator with different quantum numbers and the same frequency. Those WGMs excite the Bessel waves in the taper. The waves have different propagation constants along the Z axis and, hence, different dispersion. The initially narrow angular distribution of light in the taper broadens up with the propagation distance.

#67784 - $15.00 USD Received 6 February 2006; revised 28 March 2006; accepted 29 March 2006

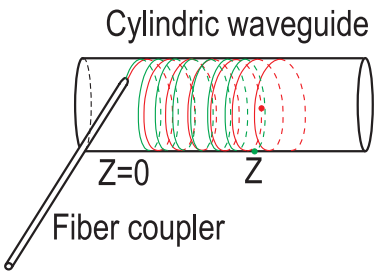

Fig. 5. To the explanation of the influence of the dispersion of the Bessel waves on azimuthal localization of light. Let us assume that the fiber coupler excites two Bessel waves shown with red and green curves in a cylindrical waveguide. The initially localized waves become azimuthally delocalized during the propagation. They cross the plane with coordinate Z at different points described by different azimuthal angles.

Let us consider a fiber coupler that excites Bessel waves with various angular moments in a cylindrical waveguide (Fig. 5). For the sake of simplicity we assume that the waveguide radius does not change and excitation of the modes is possible without a WGM resonator. The light leaving the fiber coupler is azimuthally localized. The localization disappears with distance because of the spatial dispersion of the excited modes. Results of an exact numerical simulation of the thought experiment (Fig. 5) are shown in (Fig. 6).

The longitudinal propagation constant k_z for a Bessel wave can be found from equation $k_0^2 = k_z^2 + k_l^2$ as a function of distance z and azimuthal index l:

$$k_z(z) \simeq \sqrt{k_0^2 - \left(\frac{l}{nr(z)}\right)^2}, \tag{1}$$

where $k_0 = \omega_0/c$ is the total wave vector, ω_0 is the frequency, n is the index of refraction of the material, k_l is the transverse propagation constant, and $r(z)$ is the radius.

The complex amplitude of a Bessel wave with azimuthal number l can be expressed as

$$f(r,z,\phi,l) = A_0(l,r)exp\left[j(\phi+\phi_0(l))l + j\int_0^z k_{z_1}(z_1,l)dz_1\right] \tag{2}$$

at the distance z from the beginning of the fiber taper (we assume that the radius changes adiabatically so that beams with different azimuthal numbers do not interact), where $\phi_0(l)$ and $A_0(l,r)$ are the phase and amplitude of the wave at $z = 0$.

We assume that a group of Bessel beams with the azimuthal index distributed from l_0 to $l_0 - \Delta l$ and the same frequency ω_0 is created at the beginning of the fiber. The summation of all the waves inside the dispersion interval Δl gives:

$$F(r,z,\phi,l_0,\Delta l) = \sum_{l=l_0-\Delta l}^{l_0} f(r,z,\phi,l) = \tag{3}$$

$$\sum_{l_0-\Delta l}^{l=l_0} A_0(l,r)\exp\left(j(\phi+\phi_0(l))l + j\int_0^z \sqrt{k_0^2 - \left(\frac{l}{nr(z_1)}\right)^2}dz_1\right).$$

$F(r,z,\phi,l_0,\Delta l)$ is the complex field distribution in the taper.

#67784 - $15.00 USD Received 6 February 2006; revised 28 March 2006; accepted 29 March 2006

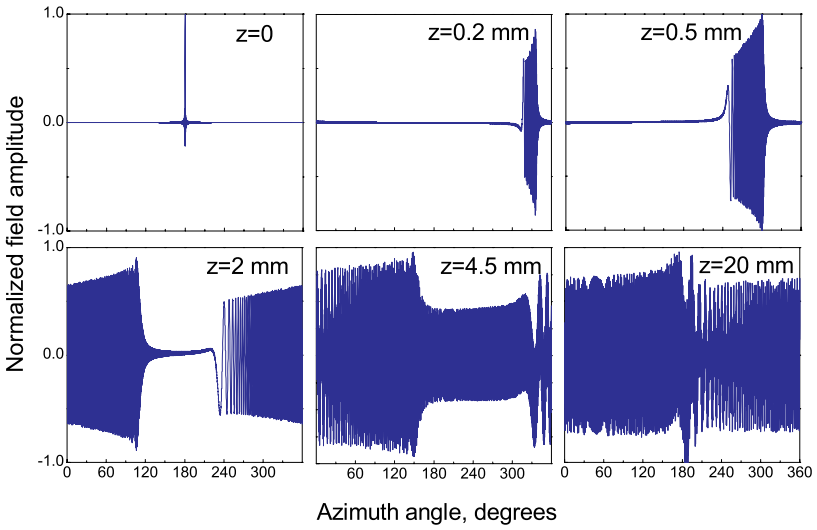

Fig. 6. Azimuthal angle distribution of the real part of the optical field at different distances from the fiber coupler. The angular width of the distribution is increasing monotonically with the distance because of the different propagation constants of the Bessel waves supported by the waveguide and having different spacial distributions and the same frequency.

To obtain Fig. 6 we have considered a tapered optical fiber with refractive index $n = 1.45$, as well as initial and final radii $r_0 = 0.3$ mm and $r_n = 1$ mm, respectively. We assumed that all the waves initially have the same phase and amplitude ($\phi_0(l) \equiv \pi$ and $A_0(l,r) \equiv 1$). Fig. 6 picture shows angular dependence of $[(F(r,z,\phi(mod(2\pi)),l_0,\Delta l) + c.c.)/2]$ for the given parameters and $l = 3000$, $\Delta l = 1000$.

The helix-shaped far field interference pattern, easily seen in Fig. 3(A), is created by the sum of all the waves at the exit of the taper. The length of the helical curve (the number of loops in the interference pattern) directly depends on the phase distribution shown in Fig. 6. For instance, if the taper is short enough, one will see the interference pattern as an unclosed helix. This is the case for a taper shorter than $z_n = 3$ mm with the other parameters as used in the simulations resulting in Fig. 6. The pattern will have at least one loop for a longer taper (see, e.g., Fig. 7).

The distribution of the far field interference pattern is determined by the Fresnel-Kirchhoff diffraction integral

$$B(x,y) = C \int_S F(x',y') e^{-ik(xx'+yy')/H} dx' dy', \tag{4}$$

where $F(x,y)$ is given by Eq. (3) at the end of the taper crossection surface (here z, l and Δl are constants), C is a constant, S is the aperture area, and H is the distance between the screen and the aperture. A direct evaluation of the integral is complicated, but we can approximate this integral by assuming that amplitudes of the particular Bessel waves ($A_0(l,r)$) are nonzero only in a thin belt close to the circumference of the taper crossection. The radial thickness of the

#67784 - $15.00 USD Received 6 February 2006; revised 28 March 2006; accepted 29 March 2006

belt is approximately $\Delta r = r_n/l^{2/3}$, as for high order WGMs. Splitting the circumference of the taper surface at small segments $1 \gg \Delta\phi \gg \lambda/(2\pi\Delta r)$, we estimate the integral as

$$B(\phi,\theta) = C_1 \int_0^{\Delta\phi} F(r = r_n - \Delta r/2, z = z_n, \phi + \phi_1, l_0, \Delta l) e^{-jk_0 r\phi_1 \sin\theta} k_0 r d\phi_1, \quad (5)$$

where $r = r_n - \Delta r/2$, C_1 is a normalization parameter. To find the optimum step $\Delta\phi_{opt}$ we first approximate the angle θ for the region of the localization of the interference pattern and take $\Delta\phi_{opt} \simeq \lambda/[2\pi(\sin\theta)\Delta r]$. For $\sin\theta \approx 0.22$ and $\Delta r \approx 4.3 \times 10^{-4}$ cm, which are the values for our taper, we get $\Delta\phi_{opt} \simeq 0.11$. The result of the optimum step calculation is shown in Fig. 7.

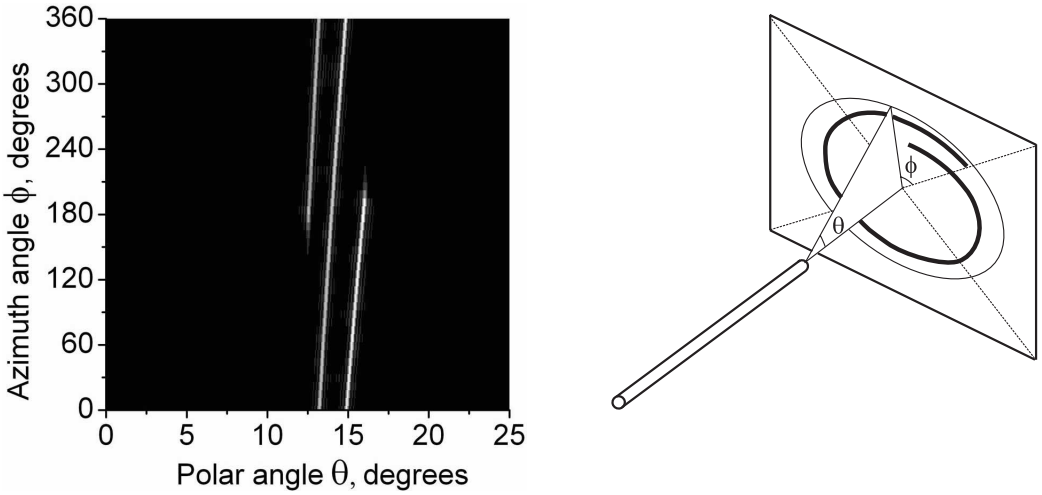

Fig. 7. Numerical simulation of the interference pattern obtained for the Bessel beams with $l = 3000$, $\Delta l = 1000$, wavelength $\lambda = 650$ nm, and $z_n = 20$ mm (see text for the explanation).

3.2. Propagation

Let us roughly estimate the propagation distance L_B for the generated Bessel beams. Because the beams can be considered as a superposition of plane waves propagating at the angle $\theta \approx \arcsin(k_l(r_n)/k_0)$ to the surface of the crossection of the taper, the propagation distance corresponds to $L_B = r_n/\mathrm{arctg}(\theta)$, where $k_l(r_n) = k_l(r_0)r_0/r_n$ and at the very beginning of the taper $k_l(r_0) = k_0$. Now the equations for the beam divergence θ and beam propagation length L_B can be written as $\theta \approx \arcsin(r_0/r_n)$ and $L_B \approx {r_n}^2/r_0$, $\theta << 1$. For parameters of our experiment $r_0 = 0.5$ mm, $r_n = 3$ mm, and $l = 7000$ we get $L_B \approx 18$ mm. At this distance the Bessel beam decays significantly, and its phase structure is very disturbed, though its momentum is still preserved. Experimental data demonstrate a Bessel beam propagation length of the same order. In order to get a distance of a meter, the exit radius of the taper should be at least seven times larger. It is difficult to reproduce such a taper experimentally using our technique of fabrication.

Let us study the divergence of a single truncated Bessel beam numerically to demonstrate the nature of the beam decay. For the sake of simplicity of the computation we consider comparably low order Bessel beams here. We take a tapered fiber with ending radius $r_n = 10\ \mu$m as a source

#67784 - $15.00 USD Received 6 February 2006; revised 28 March 2006; accepted 29 March 2006

of light. According to Huygens the complex field amplitude can be described by the diffraction integral [11]

$$B(x,y,z) = C_2 \int_S \frac{f e^{jk_0 R}}{R} ds, \tag{6}$$

where amplitude of optical field $f = J_m(k_l r)e^{-jl\phi}$, $J_m(k_l r)$ is the Bessel function of m-th order, C_2 is a scale parameter, R is the distance between point in the plane of end of the fiber and the point (x,y,z) where diffraction pattern is obtained.

In our case it is useful to employ cylindrical coordinates. The azimuth angle ϕ does not contain information on the divergence because our system is symmetrical. We can exclude it from the final consideration without any mathematical reduction. Now the diffraction integral looks like:

$$B(r,z) = C_2 \int_0^{r_0} \int_0^{2\pi} \frac{J_m(k_l r')}{R} e^{-jl\phi'} e^{-jk_0 R} r' d\phi' dr'; \;\; R = \sqrt{(r'\cos\phi' - r)^2 + (r'\sin\phi')^2 + z^2} \tag{7}$$

Please note that ϕ' coordinate appeared under integral. After selection of certain angle where the optical field is to be calculated the function under the integral loose symmetry. This diffraction integral was computed numerically for $m = 17$ and $l = 30$ as well as for $m = 10$ and $l = 15$.

Fig. (8) represents results of simulations of the field intensity $|B(r,z)|^2$ in the plane which is parallel to the fiber taper symmetry axis. The truncated Bessel beam does not change its shape but has radiative loss. This is seen as a straight Bessel beam and group of conically diverged beams in Fig. (8). Similar behavior was predicted for the zero-order Bessel-Gauss beam [10].

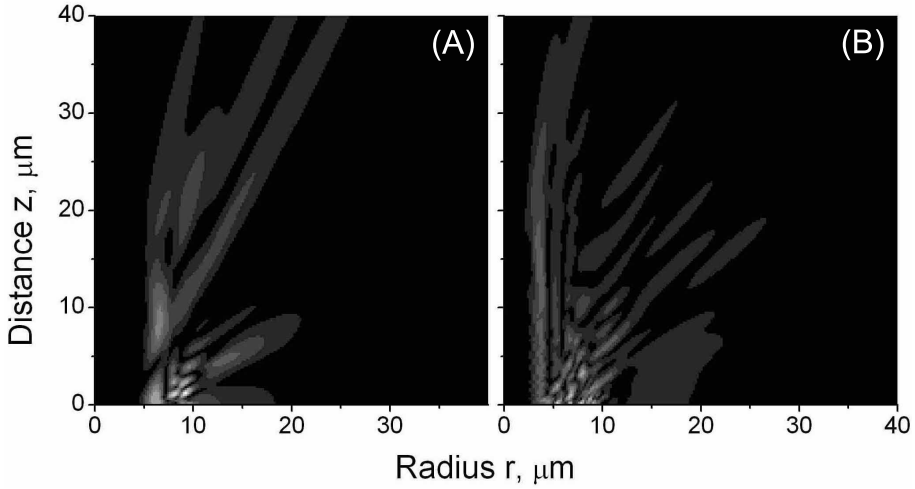

Fig. 8. Intensity pattern for the truncated Bessel beams leaving the fiber taper with 10 μm radius. The ordinate axis coincides with the symmetry axis of the taper. The pictures correspond to beams with numbers (A) $m = 17$ and $l = 30$, and (B) $m = 10$ and $l = 15$.

3.3. Shadow

We explain the shape of the shadow using principles of geometric optics. We assume that the Bessel beams are significantly truncated, such that $m \gg l - m$ and consider a one dimensional

#67784 - $15.00 USD Received 6 February 2006; revised 28 March 2006; accepted 29 March 2006

rod AA' placed at the distance h from the fiber and $H-h$ from the screen (Fig. 9). The surfaces of the fiber crossection and the screen are parallel to the rod. The point A of the rod is illuminated by the plane wave leaving point S on the fiber rim. Point B is the shadow of point A.

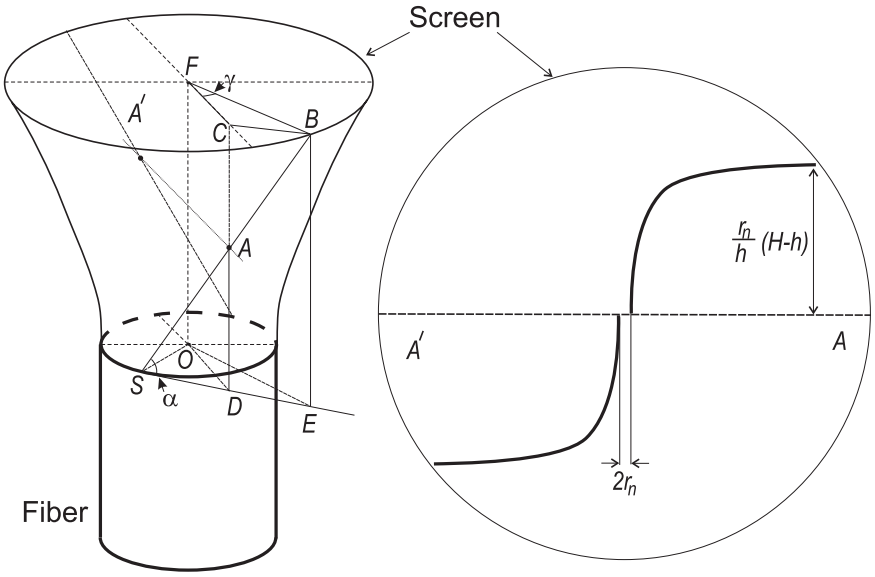

Fig. 9. Formation of the shadow (inset) of a straight rod AA' illuminated with a Bessel beam.

Let us find angle γ (angle CFB), that determines the change of the position of the shadow (B) with respect the straight projection (C) of point A of the rod. To do this we need to know all the sides of triangle CFB.

Side CF is equal to the segment OD. The line segment SAB touches the surface of the fiber so angle OSD is equal to 90^o. Segment AD is equal to h. Segment OS is equal to r_n. Angle ADS is equal to 90^o, and angle ASD is equal to α. Therefore

$$FC = \sqrt{r_n^2 + \left(\frac{h}{\mathrm{tg}\alpha}\right)^2}. \tag{8}$$

Following the same logic we find

$$FB = \sqrt{r_n^2 + \left(\frac{H}{\mathrm{tg}\alpha}\right)^2}. \tag{9}$$

To find segment CB we note that angle ACB is equal to 90^o, and angle CBA is equal to α, hence

$$CB = \frac{H-h}{\mathrm{tg}\alpha}. \tag{10}$$

Using the theorem of cosines we get

$$\cos\gamma = \frac{FC^2 + FB^2 - CB^2}{2FC \cdot FB} \rightarrow \mathrm{tg}\gamma = \frac{r_n \dfrac{H-h}{\mathrm{tg}\alpha}}{r_n^2 + \dfrac{Hh}{(\mathrm{tg}\alpha)^2}}. \tag{11}$$

#67784 - $15.00 USD Received 6 February 2006; revised 28 March 2006; accepted 29 March 2006

Angle α can be directly found from the formula $\mathrm{tg}\alpha = k_z(r_n)/k_l(r_n)$. Finally, the distance from the shadow point (B) to the direct projection of the rod AA' is equal to $FB\sin\gamma$.

Let us now assume that we generated a lot of Bessel beams with different $k_z(r_n)/k_l(r_n)$, as is done in the experiment. Each Bessel beam projects a point of the rod to different places of the screen. The complete shadow line is shown in the inset of Fig. (9). This result directly resembles our experimental observations.

4. Conclusion

Using fused silica whispering gallery mode resonators we have demonstrated the generation of optical beams with angular momentum exceeding a thousand. The beams propagate more than a centimeter in the free space. Exactly the same approach would allow efficient generating Bessel beams with momenta exceeding 10^5. Interference patterns of the multiple beams as well as the peculiar shadow pictures created with the beams are demonstrated experimentally and explained theoretically.

Acknowledgments

The research described in this paper was carried out at the Jet Propulsion Laboratory, California Institute of Technology, under a contract with the National Aeronautics and Space Administration and partial sponsorship from DARPA. A. Matsko appreciates useful discussions with V. Ilchenko and I. Marinenko.

#67784 - $15.00 USD Received 6 February 2006; revised 28 March 2006; accepted 29 March 2006